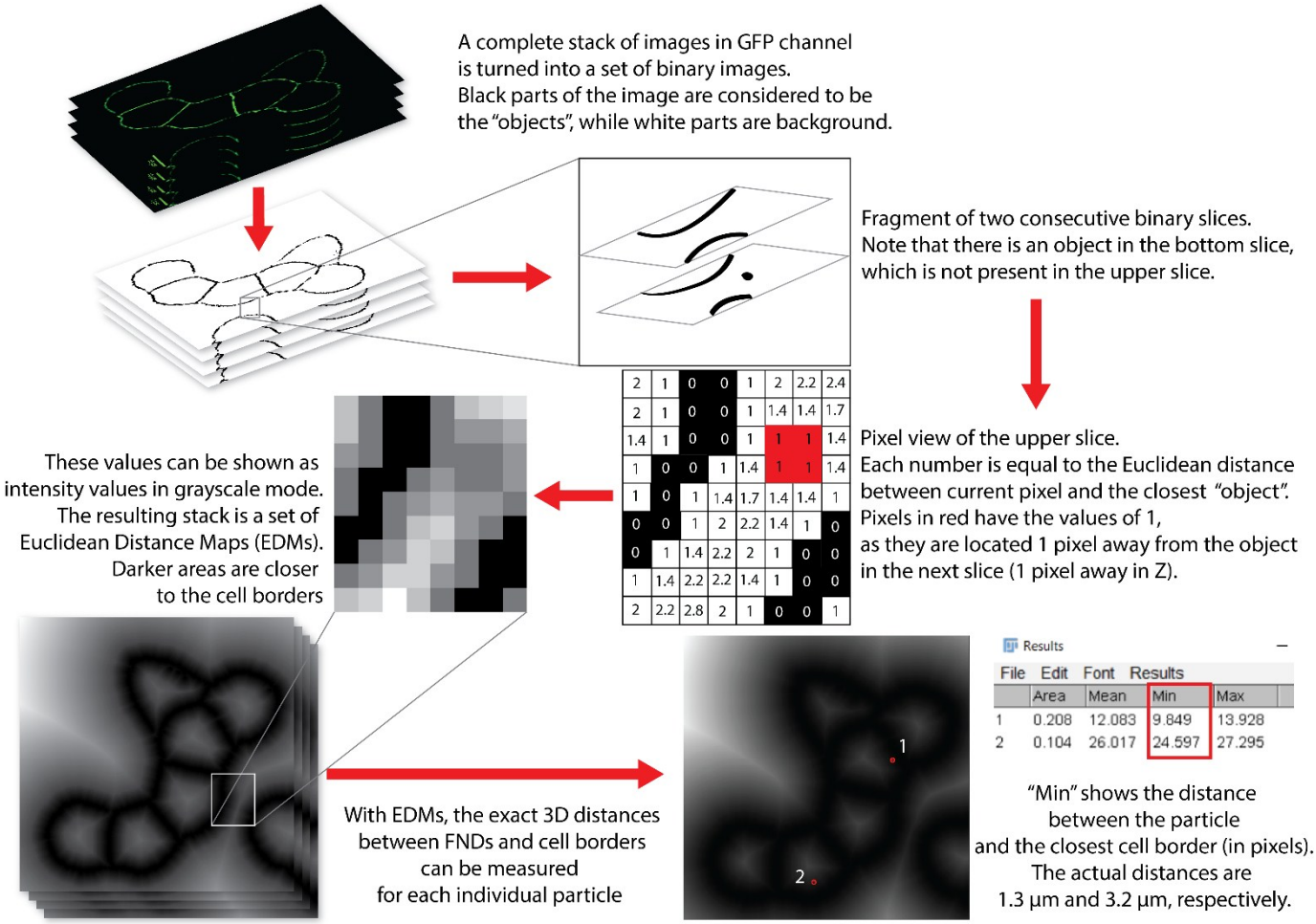

Supplementary Figure 1. Confocal image processing workflow. Data from the GFP channel are used to calculate 3D distances from the cell borders. From the resulting distance maps, we can calculate the distance between each FND and the closest cell membrane in 3D.

Statistical significance of differences in the particle distances from the membrane and the particle volumes was assessed with two-way ANOVA, with the protocol and the FND concentrations used as predictors. The results of the statistical analysis are summarized in Supplementary Tables 1 and 2. The values in the cells show the significance of the differences between the group stated on top (column names) and the group stated on the left (row names). Shades of orange represent an increase in the observed values, while shades of blue represent a decrease. Darker shadings stand for larger statistical significance. The p-values are reported as following:

- * - $p \leq 0.05$
- ** - $p \leq 0.01$
- *** - $p \leq 0.001$
- **** - $p \leq 0.0001$
- ns – not significant, $p > 0.05$

An intersection of two protocols gives a summary of all comparisons between these protocols.

Supplementary Table 1 reflects the differences in the FND uptake efficiency. For instance, protocol C yields significantly higher numbers of internalized FNDs per cell than protocol A (upper right part of table 1), except for the lowest FND concentration, where no statistically significant differences could

be found. At the same time, FND concentration has no significant impact on the number of internalized FNDs, when the particles are administered from the top (upper left part of table 1). On the other hand, there is a clear dose dependence in case of protocol B (central part of table 1) and protocol C (bottom right part of table 1).

Supplementary Table 1. Statistical significance of the differences in the number of internalized FNDs between different protocols and FND concentrations.

Experimental procedure and concentration of FNDs, µg/mL		**Protocol A (FNDs on top)**			**Protocol B (FNDs from below)**			**Protocol C (trypsin-EDTA + FNDs on top)**		
		0.5	**1**	**5**	**0.5**	**1**	**5**	**0.5**	**1**	**5**
		as compared to:								
Protocol A (FNDs on top)	**0.5**	-	ns	ns	*	****	****	ns	****	****
	1	ns	-	ns	ns	**	****	ns	****	****
	5	ns	ns	-	ns	****	****	ns	****	****
Protocol B (FNDs from below)	**0.5**	*	ns	ns	-	ns	****	ns	*	****
	1	****	**	****	ns	-	****	ns	ns	****
	5	****	****	****	****	****	-	****	****	ns
Protocol C (trypsin-EDTA + FNDs on top)	**0.5**	ns	ns	ns	ns	ns	****	-	*	****
	1	****	****	****	*	ns	****	*	-	****
	5	****	****	****	****	****	ns	****	****	-

Supplementary Table 2 reports the significance of the differences in the observed volume of FND aggregates in the same way. Protocol A, 5 µg/mL, result in significantly larger aggregates than any other combination. Both protocol A (top left part of table 2) and protocol B (central part of table 2) show a positive relation between the FND concentration and the aggregate size, whereas protocol C (bottom right part of table 2) does not.

Supplementary Table 2. Statistical significance of the differences in the observed volume of internalized FNDs between different protocols and FND concentrations.

Experimental procedure and concentration of FNDs, µg/mL		**Protocol A (FNDs on top)**			**Protocol B (FNDs from below)**			**Protocol C (trypsin-EDTA + FNDs on top)**		
		0.5	**1**	**5**	**0.5**	**1**	**5**	**0.5**	**1**	**5**
		as compared to:								
Protocol A (FNDs on top)	**0.5**	-	ns	****	ns	***	**	ns	ns	ns
	1	ns	-	****	ns	****	***	ns	ns	ns
	5	****	****	-	****	****	****	****	****	****
Protocol B (FNDs from below)	**0.5**	ns	ns	****	-	*	*	ns	ns	ns
	1	***	****	****	*	-	ns	**	****	***
	5	**	***	****	*	ns	-	*	****	**
Protocol C (trypsin-EDTA + FNDs on top)	**0.5**	ns	ns	****	ns	**	*	-	ns	ns
	1	ns	ns	****	ns	****	****	ns	-	ns
	5	ns	ns	****	ns	***	**	ns	ns	-

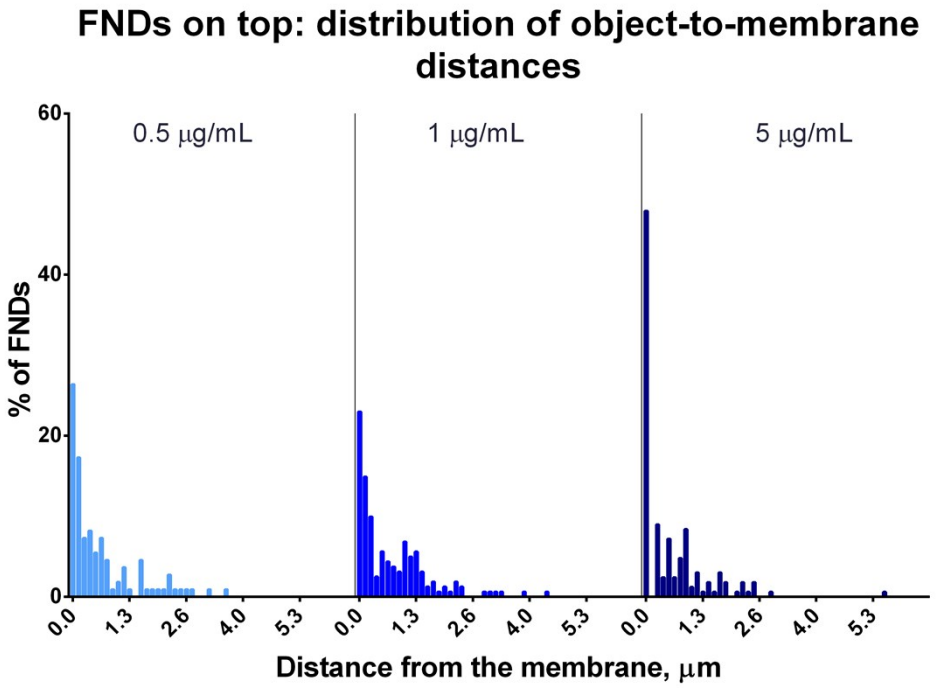

Supplementary Figure 2. Distribution of distances between internalized FNDs and the cell membranes at different concentrations of FNDs (protocol A – "FNDs on top"). Note an increase in the proportion of FNDs in the first bin (distance = 0, the object is colocalized with the membrane) in case of the highest FND concentration.

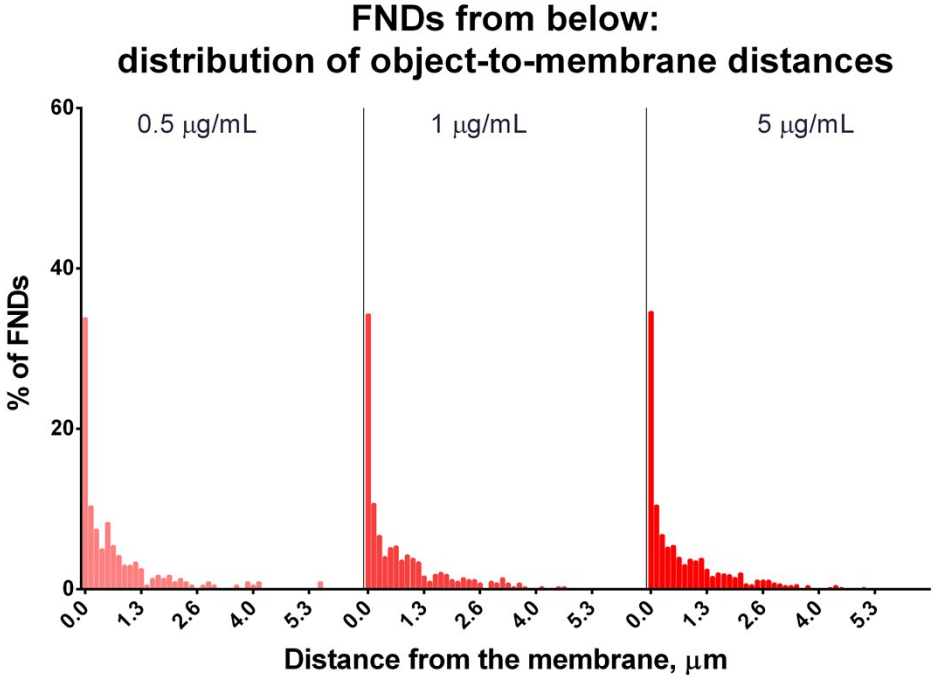

Supplementary Figure 3. Distribution of distances between internalized FNDs and the cell membranes at different concentrations of FNDs (protocol B – "FNDs from below"). Although a larger portion of FNDs is retained at the membrane, as compared to protocol A (Supplementary Figure 2), the distance distributions are not affected by increasing concentrations of FNDs.

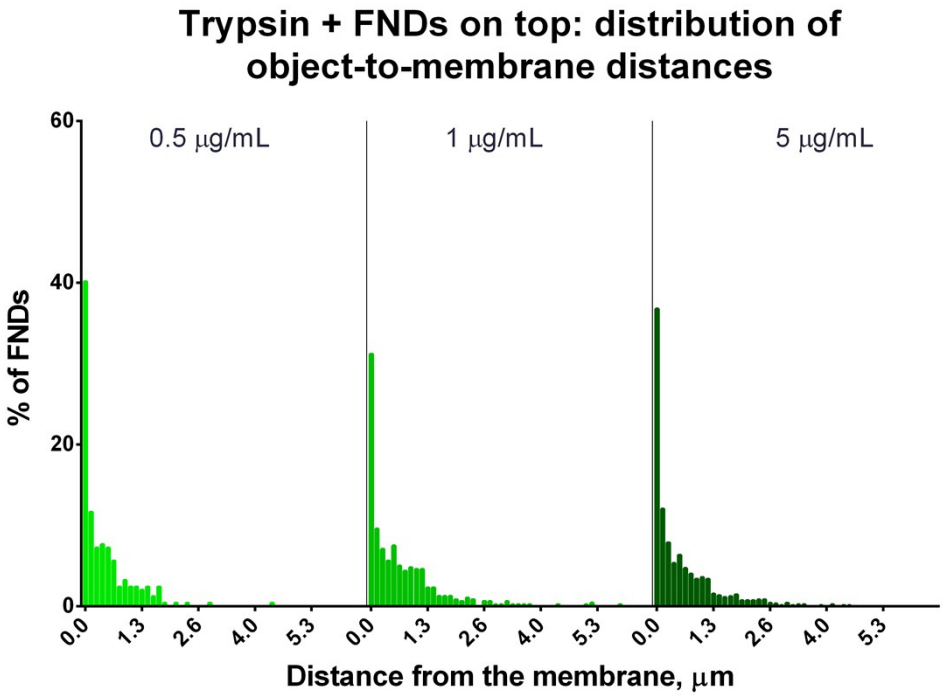

Supplementary Figure 4. Distribution of distances between internalized FNDs and the cell membranes at different concentrations of FNDs (protocol C – "trypsin + FNDs on top"). Similar to protocol B (Supplementary Figure 3), the proportion of FNDs retained at the cell membrane does not increase at higher FND concentrations.

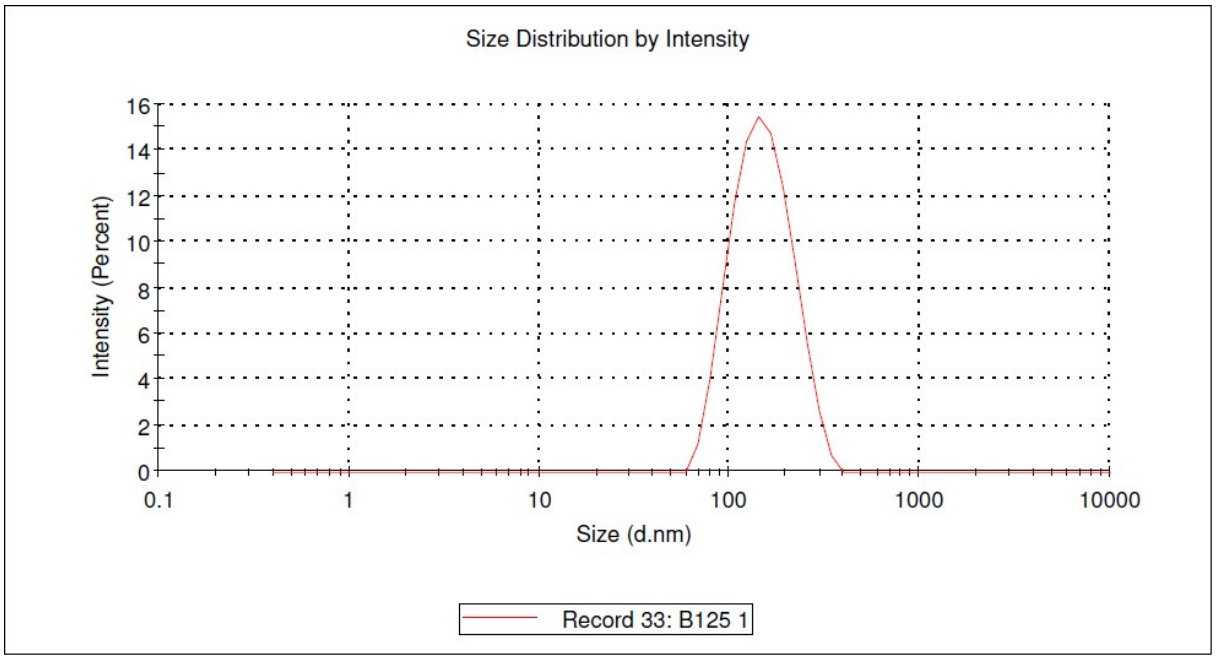

Supplementary Figure 5. Size distribution of 120 nm FNDs, measured with dynamic light scattering. Average size is 156 ± 55 nm.

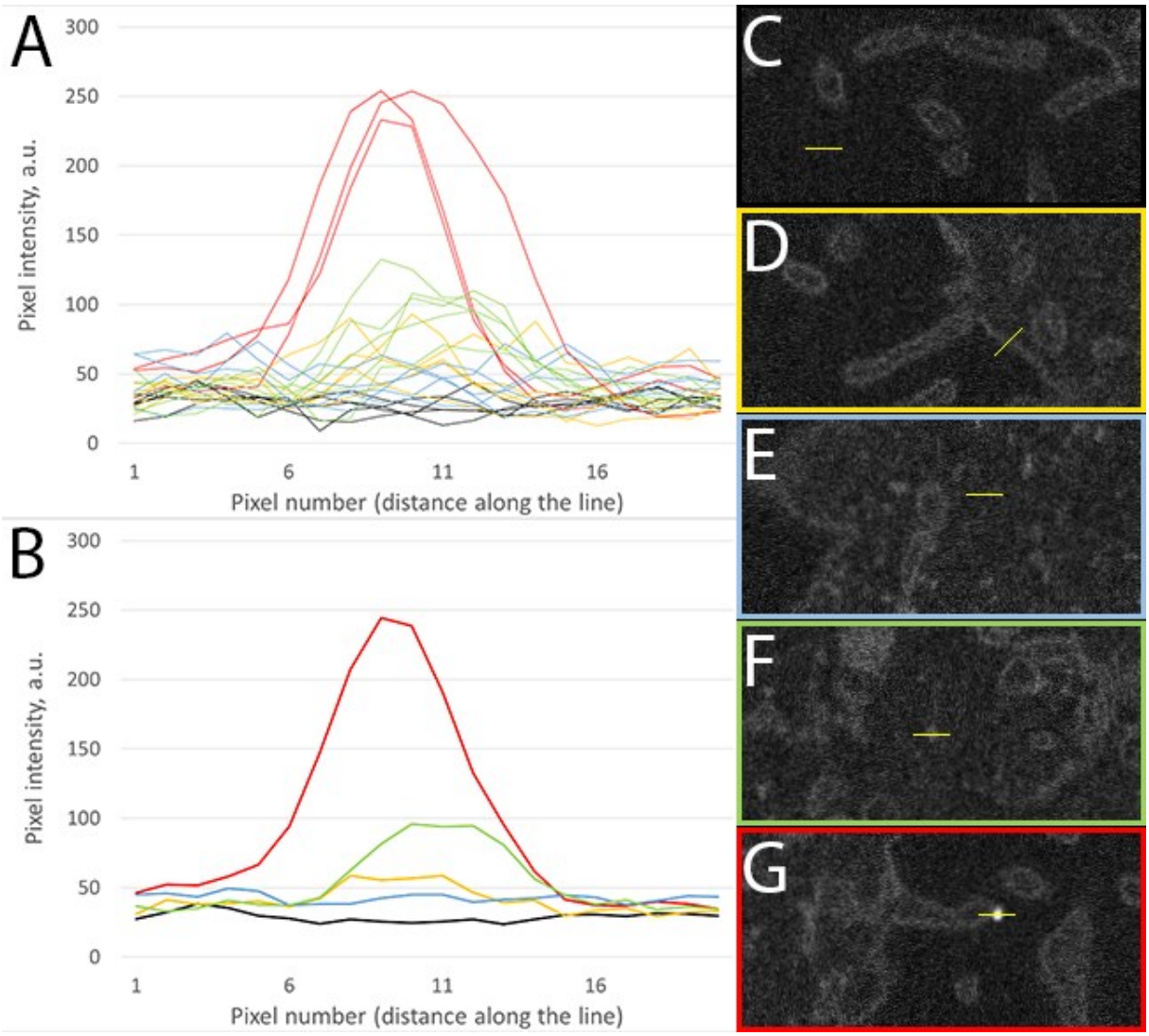

Supplementary Figure 6. (A) Intensity profiles of the FIB-SEM sections. Each profile was obtained along the length of 20 pixels (200 nm) at a random position on the section. Black curves correspond to the profiles observed in the background regions; yellow – at the cell membrane; blue – in the cytoplasmic area, free of organelles; green – across the ribosomes. Three red profiles correspond to the bright electron-dense spots, identified as nanodiamond particles. Such high peak intensity, accompanied by high contrast, is not characteristic for cellular components, such as ribosomes or protein ensembles. (B) The average intensity profiles for each group. (C-G) Sampling of intensity profiles of background (C), cell membrane (D), cytoplasm (E), ribosomes (F), nanodiamonds (G). Brightness and contrast settings are the same in all panels. The sampling lines are shown in yellow.

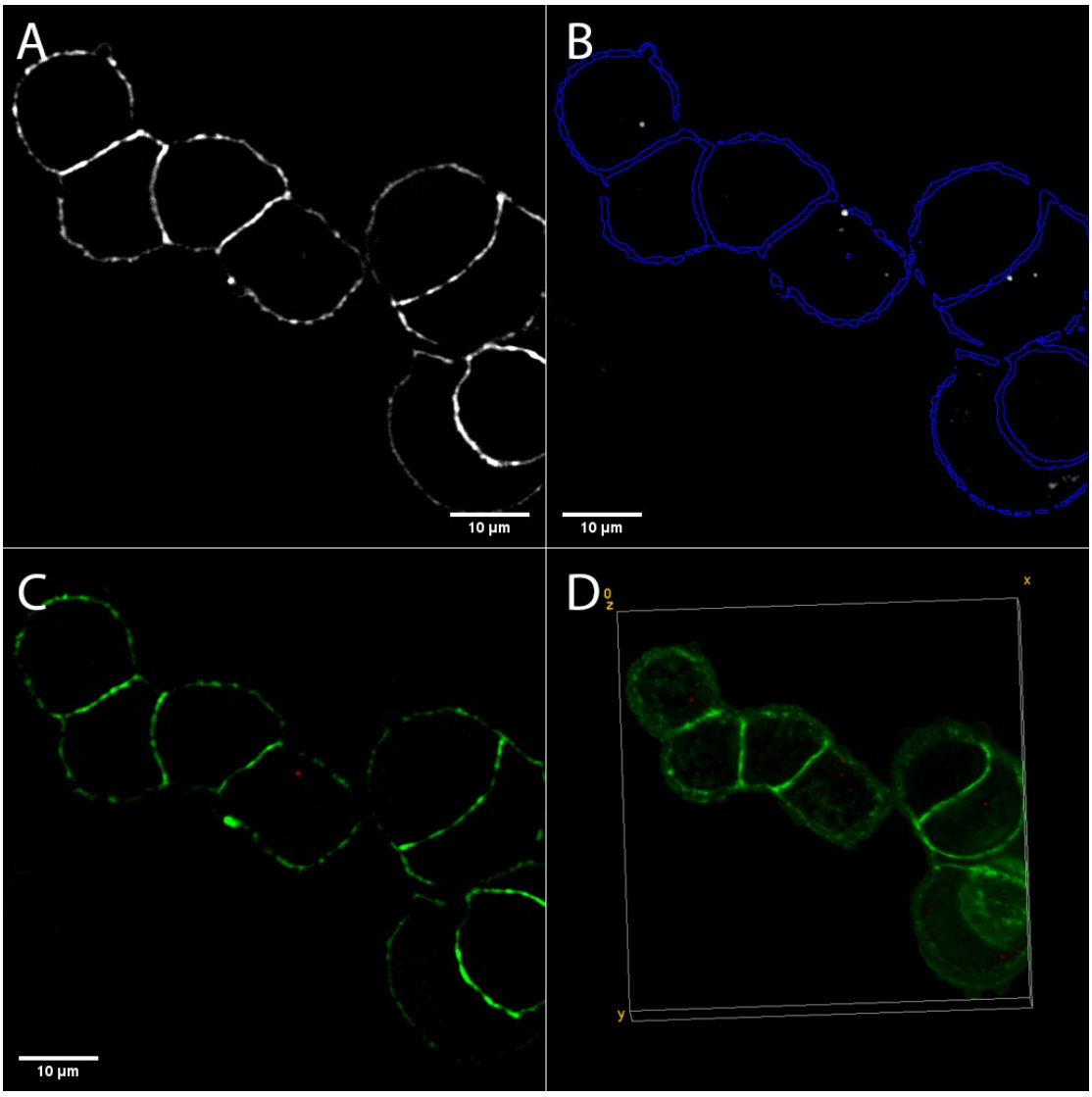

Supplementary Figure 7. Representative z-stack of HT-29 GFP-EpCAM cells, incubated with 0.5 µg/mL of FNDs, protocol A – "FNDs on top". (A) Cluster of HT-29 GFP-EpCAM cells, as seen in GFP channel. (B) Z-projection of the far-red channel reveals the internalized FNDs, located at different focal planes in the cells. Blue – cell borders, as seen in the focal plane, shown in A. (C) Overlay of GFP and FND channels (different focal plane than in A). Note that one FND can be clearly seen in the central cell, as other particles are located in other focal planes. (D) 3D-reconstruction of the HT-29 GFP-EpCAM cluster with internalized FNDs.

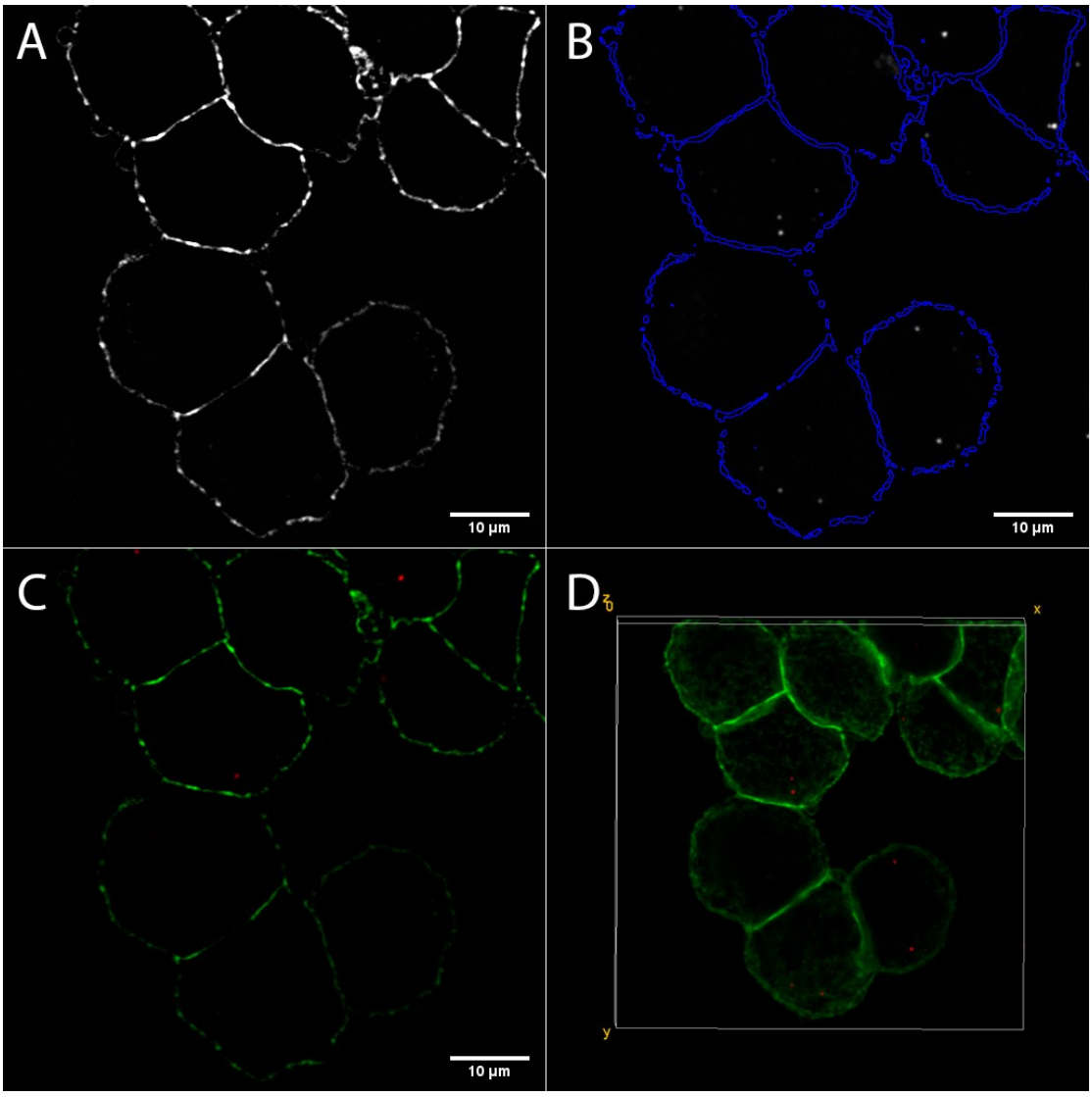

Supplementary Figure 8. Representative z-stack of HT-29 GFP-EpCAM cells, incubated with 1 µg/mL of FNDs, protocol A – "FNDs on top". (A) Cluster of HT-29 GFP-EpCAM cells, as seen in GFP channel. (B) Z-projection of the far-red channel reveals the FNDs, located at different focal planes in the cells. Blue – cell borders, as seen in the focal plane, shown in A. (C) Overlay of GFP and FND channels. (D) 3D-reconstruction of the HT-29 GFP-EpCAM cluster with internalized FNDs.

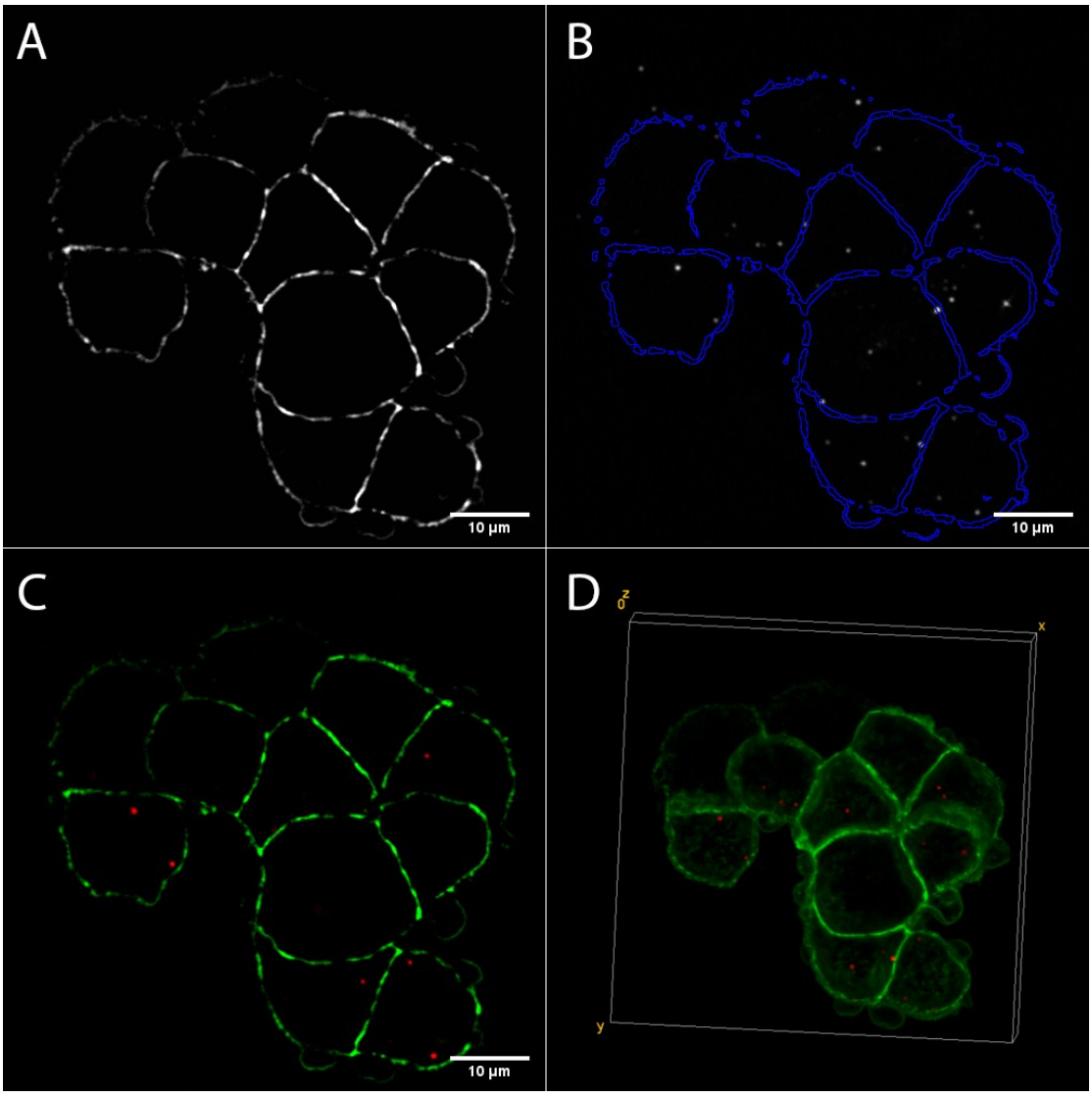

Supplementary Figure 9. Representative z-stack of HT-29 GFP-EpCAM cells, incubated with 5 µg/mL of FNDs, protocol A – "FNDs on top". (A) Cluster of HT-29 GFP-EpCAM cells, as seen in GFP channel. (B) Z-projection of the far-red channel reveals the FNDs, located at different focal planes in the cells. Blue – cell borders, as seen in the focal plane, shown in A. (C) Overlay of GFP and FND channels. (D) 3D-reconstruction of the HT-29 GFP-EpCAM cluster with internalized FNDs.

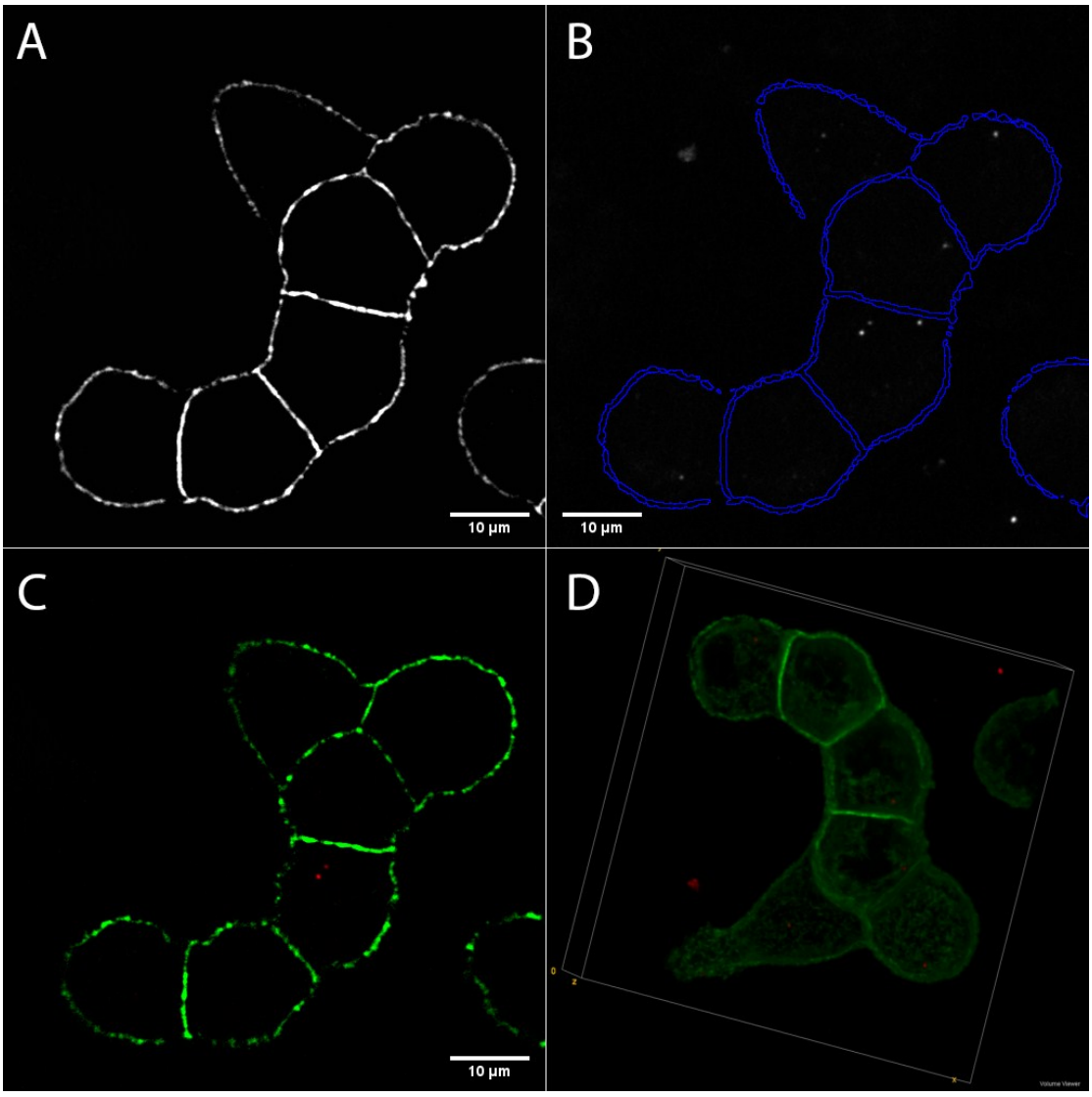

Supplementary Figure 10. Representative z-stack of HT-29 GFP-EpCAM cells, incubated with 0.5 µg/mL of FNDs, protocol B – "FNDs from the bottom". (A) Cluster of HT-29 GFP-EpCAM cells, as seen in GFP channel. (B) Z-projection of the far-red channel reveals the internalized FNDs, located at different focal planes in the cells. Blue – cell borders, as seen in the focal plane, shown in A. (C) Overlay of GFP and FND channels (different focal plane than in A). Note that only two FNDs can be clearly seen in the central cell, as other particles are located in other focal planes. (D) 3D-reconstruction of the HT-29 GFP-EpCAM cluster with internalized FNDs.

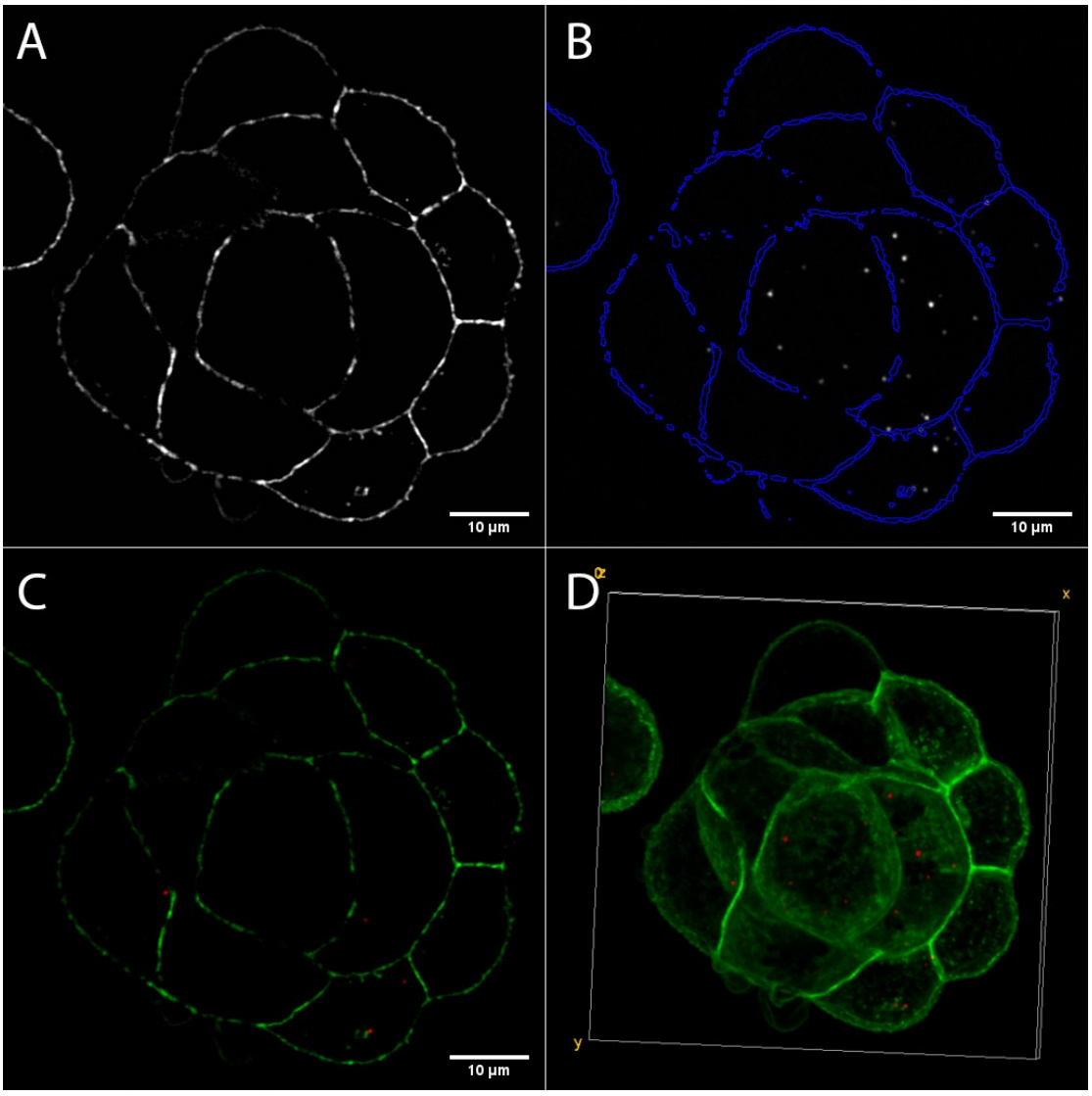

Supplementary Figure 11. Representative z-stack of HT-29 GFP-EpCAM cells, incubated with 1 µg/mL of FNDs, protocol B – "FNDs from the bottom". (A) Cluster of HT-29 GFP-EpCAM cells, as seen in GFP channel. (B) Z-projection of the far-red channel reveals the internalized FNDs, located at different focal planes in the cells. Blue – cell borders, as seen in the focal plane, shown in A. (C) Overlay of GFP and FND channels. (D) 3D-reconstruction of the HT-29 GFP-EpCAM cluster with internalized FNDs.

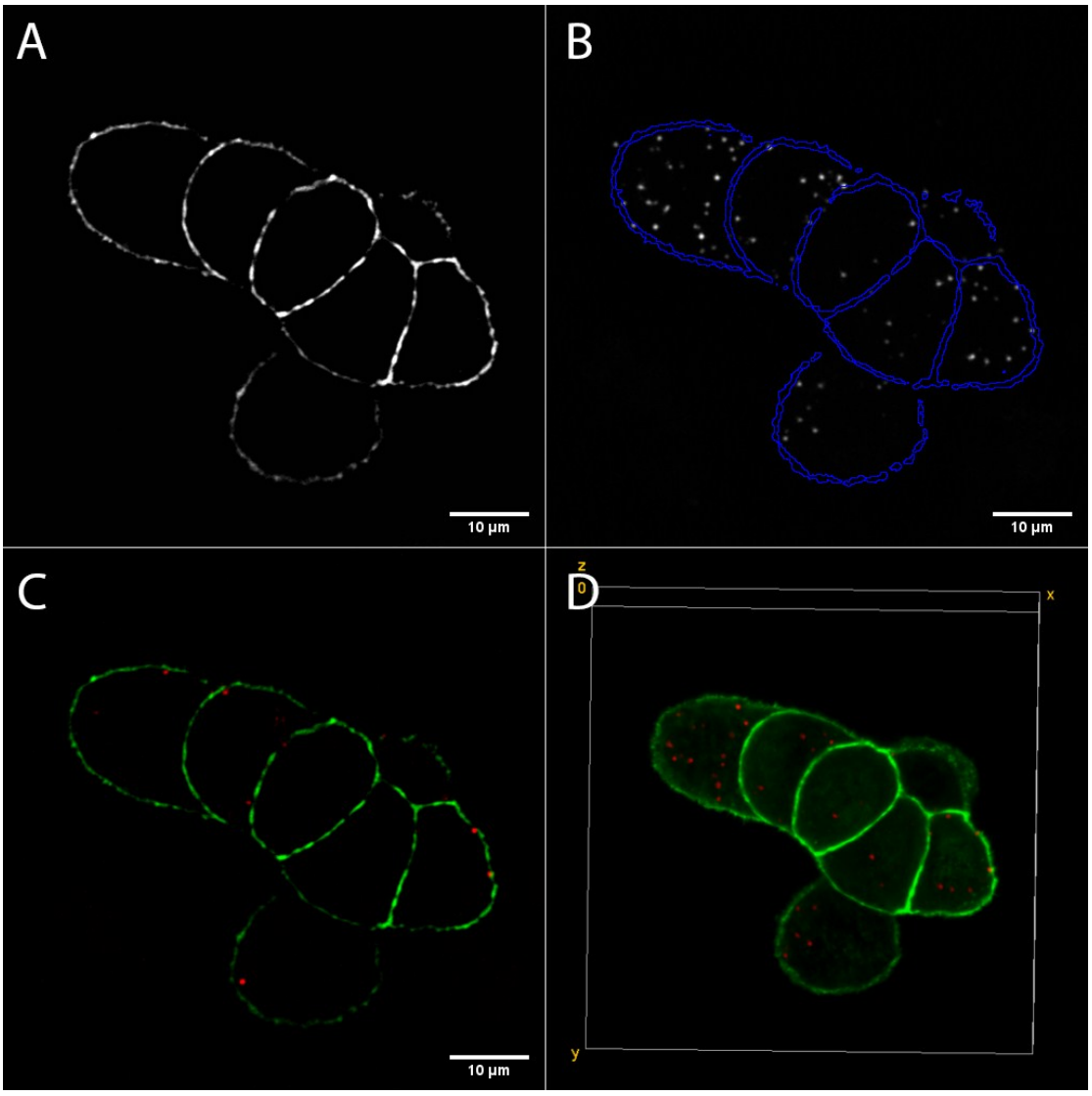

Supplementary Figure 12. Representative z-stack of HT-29 GFP-EpCAM cells, incubated with 5 µg/mL of FNDs, protocol B – "FNDs from the bottom". (A) Cluster of HT-29 GFP-EpCAM cells, as seen in GFP channel. (B) Z-projection of the far-red channel reveals the internalized FNDs, located at different focal planes in the cells. Blue – cell borders, as seen in the focal plane, shown in A. (C) Overlay of GFP and FND channels. (D) 3D-reconstruction of the HT-29 GFP-EpCAM cluster with internalized FNDs.

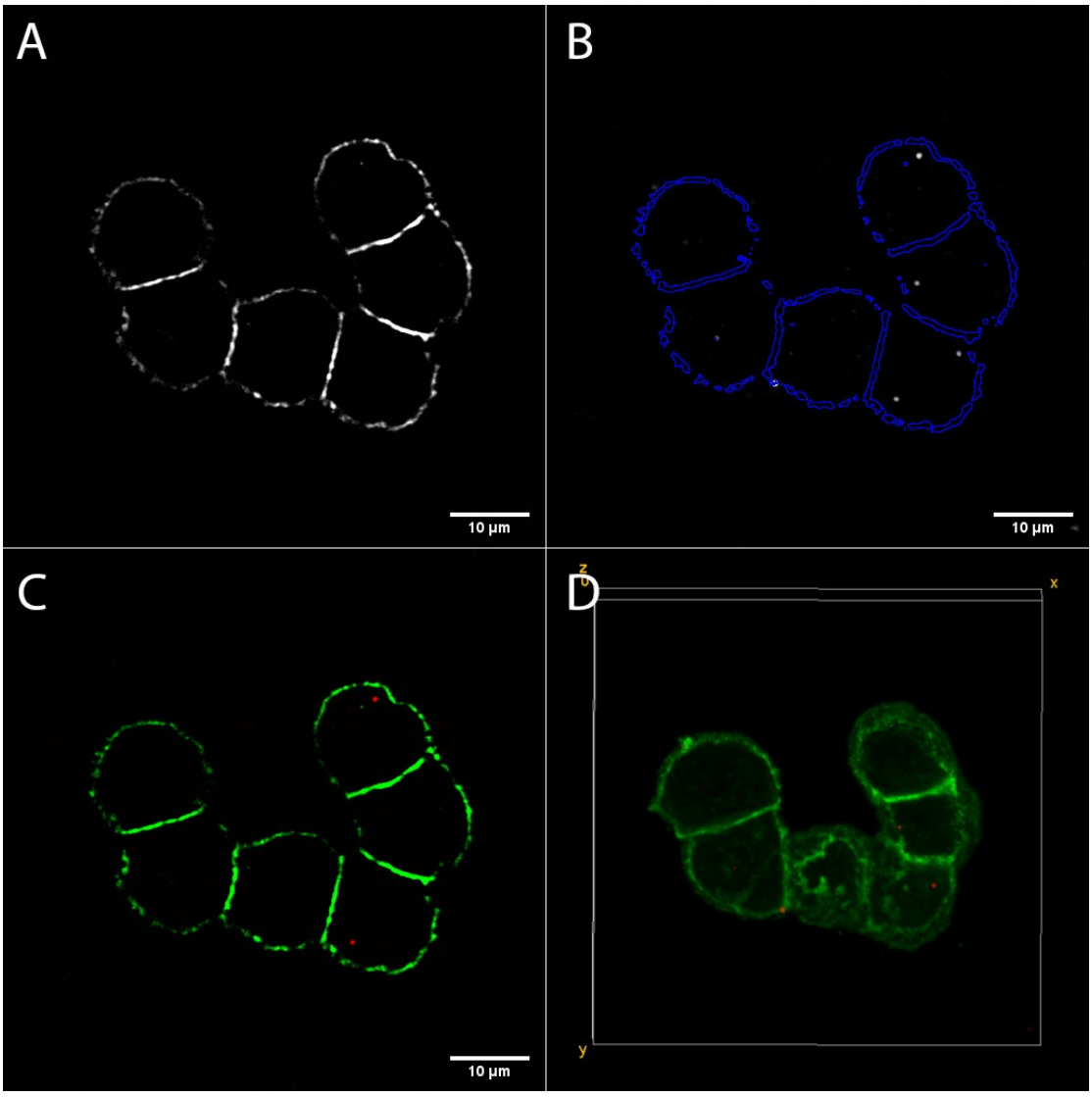

Supplementary Figure 13. Representative z-stack of HT-29 GFP-EpCAM cells, incubated with 0.5 µg/mL of FNDs, protocol C – "trypsin-EDTA + FNDs on top". (A) Cluster of HT-29 GFP-EpCAM cells, as seen in GFP channel. (B) Z-projection of the far-red channel reveals the internalized FNDs, located at different focal planes in the cells. Blue – cell borders, as seen in the focal plane, shown in A. (C) Overlay of GFP and FND channels. (D) 3D-reconstruction of the HT-29 GFP-EpCAM cluster with internalized FNDs.

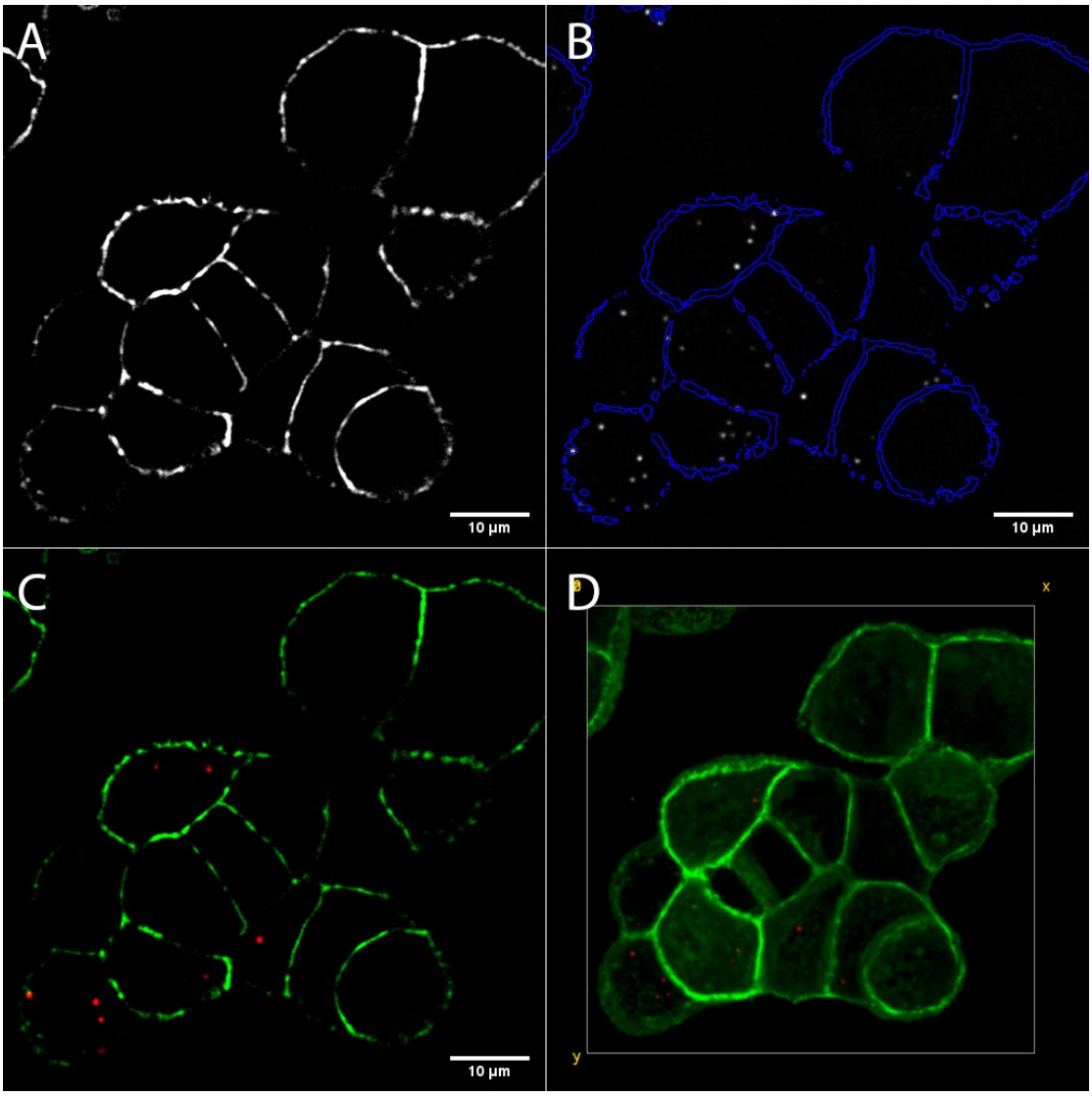

Supplementary Figure 14. Representative z-stack of HT-29 GFP-EpCAM cells, incubated with 1 µg/mL of FNDs, protocol C – "trypsin-EDTA + FNDs on top". (A) Cluster of HT-29 GFP-EpCAM cells, as seen in GFP channel. (B) Z-projection of the far-red channel reveals the internalized FNDs, located at different focal planes in the cells. Blue – cell borders, as seen in the focal plane, shown in A. (C) Overlay of GFP and FND channels. (D) 3D-reconstruction of the HT-29 GFP-EpCAM cluster with internalized FNDs.

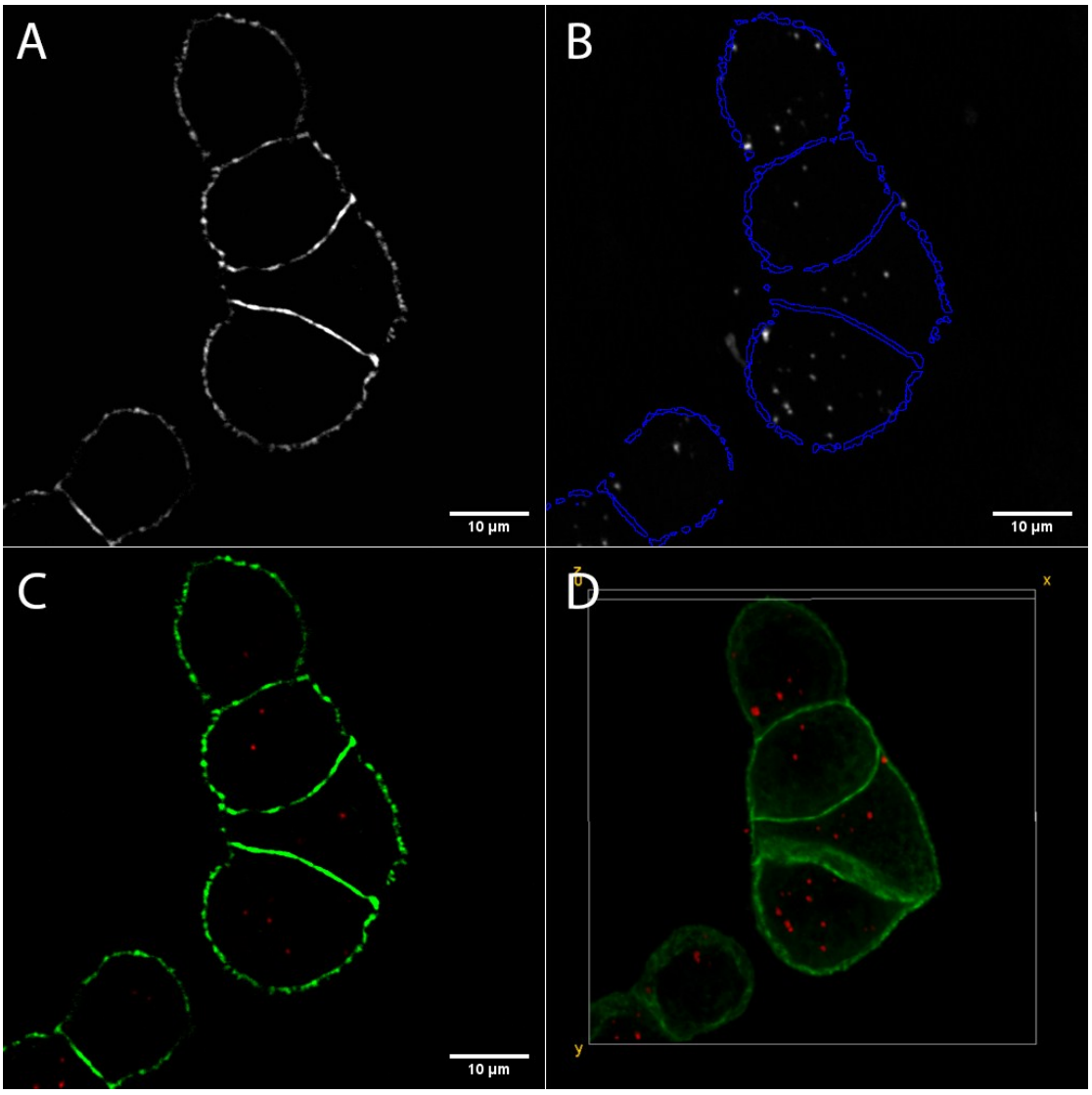

Supplementary Figure 15. Representative z-stack of HT-29 GFP-EpCAM cells, incubated with 5 µg/mL of FNDs, protocol C – "trypsin-EDTA + FNDs on top". (A) Cluster of HT-29 GFP-EpCAM cells, as seen in GFP channel. (B) Z-projection of the far-red channel reveals the internalized FNDs, located at different focal planes in the cells. Blue – cell borders, as seen in the focal plane, shown in A. (C) Overlay of GFP and FND channels. (D) 3D-reconstruction of the HT-29 GFP-EpCAM cluster with internalized FNDs.